



1 **The sensitivity of benzene cluster cation chemical ionization mass spectrometry to select**
2 **biogenic terpenes**

3 Avi Lavi^{1,2}, Michael P. Vermeuel¹, Gordon A. Novak¹, Timothy H. Bertram^{1,*}

4 ¹Department of Chemistry, University of Wisconsin, Madison, WI 53706, USA;

5 ²Now at: Department of Chemistry, University of California-Riverside, Riverside, CA 92521,
6 USA;

7
8 *Correspondence to: T.H. Bertram, timothy.bertram@wisc.edu

9
10 **Abstract**

11 Benzene cluster cations are a sensitive and selective reagent ion for chemical ionization of select
12 biogenic volatile organic compounds. We have previously reported the sensitivity of a field
13 deployable chemical ionization time-of-flight mass spectrometer (CI-ToFMS), using benzene
14 cluster cation ion chemistry, for detection of dimethyl sulfide, isoprene and alpha pinene. Here,
15 we present laboratory measurements of the sensitivity of the same instrument to a series of
16 terpenes, including isoprene, α -pinene, β -pinene, D-limonene, ocimene, β -myrcene, farnesene, α -
17 humulene, β -caryophyllene and isolongifolene at atmospherically relevant mixing ratios (< 100
18 pptv). In addition, we determine the dependence of CI-ToFMS sensitivity on the reagent ion
19 neutral delivery concentration, the instrument electric field strength and water vapor concentration.
20 We show that isoprene is primarily detected as an adduct ($C_5H_8 \cdot C_6H_6^+$) with a sensitivity ranging
21 between 4-10 ncps ppt⁻¹, that depends strongly on the reagent ion precursor concentration, de-
22 clustering voltages, and specific humidity (SH). Monoterpenes are detected primarily as the
23 molecular ion ($C_{10}H_{16}^+$) with an average sensitivity, across the five measured compounds, of $14 \pm$
24 3 ncps ppt⁻¹ for SH between 7 and 14 g kg⁻¹, typical of the boreal forest during summer.
25 Sesquiterpenes are detected primarily as the molecular ion ($C_{15}H_{24}^+$) with an average sensitivity,
26 across the four measured compounds, of 9.6 ± 2.3 ncps ppt⁻¹ that is also independent of specific
27 humidity. Comparable sensitivities across broad classes of terpenes (e.g., monoterpenes and
28 sesquiterpenes), coupled to the limited dependence on specific humidity, suggests that benzene
29 cluster cation CI-ToFMS is suitable for field studies of biosphere-atmosphere interactions.

30

31



32 1. Introduction

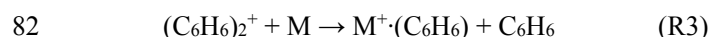
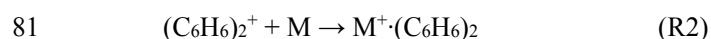
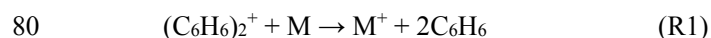
33 The annual global emission of biogenic volatile organic compounds (BVOCs) is estimated at 1000
34 TgC yr⁻¹ and exceeds the total VOC emissions from anthropogenic activities (Guenther et al.,
35 2012). Foliage emissions account for 90% of global BVOC emissions, of which isoprene (C₅H₈),
36 monoterpenes (MTs; C₁₀H₁₆) and sesquiterpenes (SQTs; C₁₅H₂₄) are the primary constituents
37 (Guenther et al., 1995). The emission rate and the chemical composition of emitted BVOCs is a
38 complex function of the vegetation species and the wide array of stress factors that it is exposed to
39 (Hallquist et al., 2009; Lang-Yona et al., 2010; Zhao et al., 2017). Atmospheric oxidation of
40 BVOCs results in the formation of low volatility compounds that can lead to new particle
41 formation (Jokinen et al., 2015; Kirkby et al., 2016) and particle growth through secondary organic
42 aerosol formation (Allan et al., 2006; Wiedensohler et al., 2009). Both of these processes impact
43 Earth's radiative budget by scattering solar radiation and/or altering cloud formation and
44 precipitation (Chung et al., 2012). The contribution of different types of BVOCs (e.g., isoprene,
45 MTs and SQTs) to secondary organic aerosols (SOA) differ significantly (Zhao et al., 2017).
46 Therefore, uncertainties in BVOCs emissions present significant issues in estimating net climate
47 forcing (Kerminen et al., 2005; Kulmala et al., 2004). Identification of the chemical composition
48 of the emitted BVOCs and quantification of the surface exchange rates of these compounds are
49 essential for understanding complex and non-linear biosphere-atmosphere interactions.

50 Chemical ionization mass spectrometry (CIMS) is a commonly utilized selective and sensitive
51 method for *in situ* detection of trace gases (Huey, 2007). The sensitivity and selectivity towards a
52 specific compound or class of compounds having similar functional groups rely on the selection
53 of an appropriate ion (i.e. reagent ion) that reacts with and ionizes the analyte *via* an ion-molecule
54 reaction. For example, iodide ions have been used to measure reactive nitrogen compounds,
55 halogen containing species and oxygenated VOCs (Lopez-Hilfiker et al., 2015; Riedel et al., 2012;
56 Thornton et al., 2010), CF₃O⁺ has been used for the detection of peroxides and organic nitrates
57 (Crounse et al., 2006), NO⁺ has been used for the selective detection of primary alcohols and
58 alkenes (Hunt and Harvey, 1975; Hunt et al., 1982), H₃O⁺ for VOCs and their oxygenated products
59 (Lindinger et al., 1998) and benzene cluster cations for dimethyl sulfide (DMS), isoprene, and
60 terpenes (Kim et al., 2016; Leibrock and Huey, 2000).



61 The benzene cation clusters spontaneously with neutral benzene *via* attractive, non-covalent
62 interactions (Chipot et al., 1996; Grover et al., 1987). Leibrock and Huey (2000) and recently Kim
63 et al. (2016) demonstrated that select VOCs including isoprene, MTs, SQTs and aromatic
64 compounds can be ionized by benzene cation clusters. Kim et al. studied the parameters that
65 control the benzene cation cluster distribution $(\text{C}_6\text{H}_6)^+(\text{C}_6\text{H}_6)_n$ at the operational conditions of the
66 CI-ToFMS, concluding that, for the specific operating conditions used, the reagent ion within the
67 ion-molecule reaction chamber was primarily in the form of the benzene dimer or larger clusters
68 (Kim et al., 2016). This conclusion is in agreement with studies showing that the dissociation
69 energy of the benzene cation dimer is significantly higher than that of the trimer or larger benzene
70 cation clusters (Krause et al., 1991), suggesting that ionization in the CI-ToFMS by benzene cluster
71 cations proceeds primarily through clusters that are at least the size of the benzene cation dimer.

72 The ionization mechanism for a given analyte (M) with the benzene cation dimer, depends on the
73 ionization energy (IE) of the analyte. Charge transfer (R1) is expected to be the dominant reaction
74 for analytes having ionization energies smaller than the benzene dimer (8.69 eV) (Grover et al.,
75 1987). In cases when the analyte IE is higher than that of benzene cation dimer, charge transfer is
76 thermodynamically unfavored and adduct formation (R2) or ligand exchange (R3) are the sole
77 modes of ionization. The ligand exchange product (R3) was previously reported for isoprene,
78 dimethyl sulfide and select alkenes, however the reaction pathway is not known (Kim et al., 2016;
79 Leibrock and Huey, 2000).



83 The low IE of benzene clusters (8.69 eV for the dimer and even smaller for larger benzene cation
84 clusters) (Grover et al., 1987; Shinohara and Nishi, 1989) is a major advantage in the quantification
85 of monoterpenes or larger volatile organic compounds such as sesquiterpenes. The IE of these
86 compounds is slightly smaller than that of the benzene dimer (e.g. 8.3 eV for β -caryophyllene
87 (Novak et al., 2001)) and the minimal excess energy in charge transfer reactions results in limited
88 fragmentation. For example, approximately 60% of β -caryophyllene was detected in its molecular



89 ionic form (M^+) in comparison to significant fragmentation observed by proton transfer reaction
90 mass spectrometry (PTR-MS) (Kim et al., 2014; Kim et al., 2009).

91 The field deployable CIMS that utilizes a time-of-flight mass analyzer (ToFMS), previously
92 described by Kim et al. combines the efficient production and transmission of ions at high pressure
93 (e.g. 75 mbar) with the high ion duty cycle of orthogonal extraction ToFMS (Bertram et al., 2011).
94 This instrument configuration is highly sensitive and capable of measuring and logging mass
95 spectra (10-800 m/Q) at rates higher than 10 Hz (Bertram et al., 2011). These benefits make CI-
96 ToFMS highly applicable for studying atmospheric exchange processes of trace gases at the air-
97 ocean interface that require fast response rates (Kim et al., 2014). However, at these pressures, the
98 distribution of benzene clusters and their associate ion-molecule reactions times are not well
99 constrained. Unlike PTR-MS, it is not possible to directly derive the analyte mixing ratio from
100 laboratory studies of the ion-molecule kinetics (reaction rates) that are conducted at lower pressure
101 in which both the reaction times and cluster distribution have been previously determined. As such,
102 quantitative analysis of atmospheric trace gases using high pressure CIMS necessitates either a
103 direct or empirical calibration for each analyte as a function of the atmospheric conditions (e.g.
104 humidity or temperature).

105 In what follows, we build on earlier studies in our group (Kim et al., 2016), which described the
106 use of benzene cluster cations as a reagent ion for the detection and quantification of dimethyl
107 sulfide, isoprene, and α -pinene. At the time of Kim et al. (2016), it was not known if: 1)
108 $C_6H_6(C_6H_6)_n^+$ ion chemistry was equally sensitive to all monoterpene compounds, 2) the
109 dependence of CI-ToFMS sensitivity on specific humidity for a broad range of monoterpenes and
110 sesquiterpenes, and 3) the source of organic impurities in the reagent ion delivery. Here, we address
111 each of these topics.

112 In this paper, we describe a high purity liquid benzene source, which permits operation of the CI-
113 ToFMS at higher reagent ion concentrations. We discuss the sensitivity of benzene cluster cation
114 chemistry to a select number of terpenes at atmospherically relevant mixing ratios (<500 pptv).
115 We report on the effect of atmospheric water vapor and the neutral benzene reagent ion precursor
116 concentration on CI-ToFMS sensitivity to select terpenes (isoprene, α - and β -pinene, D-limonene,
117 β -myrcene, ocimene, farnesene, isolongifolene, α -humulene and β -caryophyllene). We
118 demonstrate the effect of a new set of applied voltages with softer de-clustering power on the



119 observed cluster distribution in the instrument and discuss the effects of the RF only quadrupole
120 on ion transmission and its contribution to the de-clustering power of the instrument.

121 **2. Experimental**

122 2.1 Materials

123 The following analytes were purchased from Sigma-Aldrich and used with no further purification:
124 isoprene, α -pinene, β -pinene, D-limonene ($\geq 99\%$), β -myrcene (96.2%), ocimene (97.0%, as a
125 mixture of isomers), farnesene ($>90.0\%$, as a mixture of isomers) α -humulene ($>96.5\%$), β -
126 caryophyllene ($\geq 98.5\%$), isolongifolene ($\geq 98.0\%$, as a mixture of isomers), benzene ($\geq 99.5\%$) and
127 chloroform-d (99.8 atom % D). A compressed gas cylinder of 0.184 ppm of DMS-d₃ in N₂ was
128 purchased from Praxair, USA. Water was supplied from a Milli-Q system at 18.2 M Ω -cm.
129 Nitrogen was used from a UHP liquid N₂ dewar (Airgas). UHP (99.999%) oxygen cylinders were
130 purchased from Airgas.

131 2.2 Chemical Ionization Mass Spectrometer

132 The detailed description of the CI-ToFMS (Tofwerk AG, Switzerland and Aerodyne Research
133 Inc., USA) and its performance are discussed in Bertram et. al. (Bertram et al., 2011) In brief,
134 reagent ions are generated by passing 10 sccm of UHP N₂ over the headspace of a liquid benzene
135 reservoir contained in a stainless steel bottle. Benzene vapor is diluted with 2.2 slpm of N₂, prior
136 to delivery to the ²¹⁰Po source. The benzene vapor mixing ratio is estimated from the dilution ratio
137 and benzene vapor pressure. In the experiments discussed here, we varied the benzene
138 concentration between 60 and 360 ppm. A combination of stainless steel and Teflon tubing was
139 used to transfer benzene vapors to minimize extraction of organic compounds from the tubing.
140 Following dilution, benzene vapor flows through a 10 mCi α emitting radioactive ²¹⁰Po source
141 (NRD 2021–1000). The collision of α -particles with N₂ results in the formation of N₂⁺ ions that
142 ionize the benzene clusters (Dondes et al., 1966). The analyte sample is mixed with the formed
143 benzene cluster cations at the ion-molecule reactor (IMR) held at 75mbar. At this pressure, the
144 estimated analyte residence time in the IMR is 100 ms. The reagent and product ions are
145 transmitted from the IMR chamber into a collisional dissociation chamber (CDC, P=2 mbar)
146 equipped with a RF only ion-guide quadrupole, followed by a subsequent chamber (P=1.4 x 10⁻²
147 mbar) in which a second RF-only quadrupole is used to focus the ion beam. The ion beam is then



148 guided by a further set of ion optics to the entrance point of the extraction region of the compact
149 time of flight mass analyzer (Tofwerk AG, Switzerland).

150 2.3 Liquid Calibration Unit

151 A custom liquid calibration system was developed to deliver known, atmospherically relevant
152 mixing ratios (< 500 pptv) of gas-phase terpenes to the CI-ToFMS. The liquid calibration system
153 uses a syringe pump to continuously evaporate known quantities of solution into a heated carrier
154 gas flow, generating known mixing ratios of select terpenes. To produce trace concentrations of
155 each analyte, the standard liquid material was diluted in-series with chloroform-d using a set of
156 calibrated auto pipettes. Chloroform-d was chosen due to its solvent properties and low boiling
157 point (61°C) that enhances the evaporation of the analyte. Due to its ionization energy (IE > 11 eV
158 (Bieri et al., 1981)), higher than that of benzene cation clusters, it was expected that chloroform
159 would not be ionized and would have negligible impact on the benzene cluster cation ionization
160 mechanisms. To assess this, mass spectra were recorded for solutions containing solely deuterated
161 chloroform for a variety of different pump flows from 0 to 5 μl min⁻¹. We did not observe the
162 molecular cation of chloroform-d (CDCl₃⁺, 120 *m/Q*) and only very small signatures of the
163 fragments (at 48, 84 or 86 *m/Q*) were observed (Figure 1), consistent with the IE of chloroform-d
164 being higher than that of the reagent ions (11.37 ± 0.02 eV compared with 8.69 eV) (Grover et al.,
165 1987) (Werner et al., 1974). It was also determined that concentration of deuterated chloroform
166 did not interfere with reagent ion or water cluster signal intensities.

167 To evaporate the analyte solution, a controlled amount (0-5 μl min⁻¹) of the analyte solution was
168 delivered by a syringe pump (Harvard Apparatus, model 11) *via* PEEK tubing (Upchurch
169 scientific) into a heated carrier stream resulting in CDCl₃ mixing ratios from 60-300 ppmv. A
170 synthetic 80:20 N₂:O₂ mixture was used as zero air and heated by an in-line gas heater (Omega,
171 AHP-3741). The temperature of the zero air flow at the point of intersection with the PEEK tubing
172 was kept at 80°C via a PID temperature controller (Omega, CN9300). Excess zero air flow was
173 used to ensure an overflow of the CIMS inlet. The trace concentration of the evaporated analytes
174 and the elevated temperature in front of the inlet (ca. 50°C) helped to prevent re-condensation of
175 the analyte on the inlet tubing. Humidified zero air was generated by passing a fraction of the total
176 flow through the head space of a water reservoir. The relative humidity (RH) of the total air flow



177 was measured using a relative humidity sensor (Vaisala, HMP110), calibrated using the procedure
178 described in Greenspan (1977).

179 The sensitivities reported in this paper are presented in normalized counts per second per pptv
180 ($\text{ncps} \cdot \text{pptv}^{-1}$). We normalized the analyte ion count-rates by the sum of the benzene cation
181 monomer ($78 m/Q$) and dimer ($156 m/Q$) count rates to a reference of 1×10^6 counts per second of
182 total reagent ion signal in order to account for changes in ion transmission and generation over
183 time. Sensitivities are calculated as the slope of the linear fit of each calibration curve of 5-7 steps
184 (

185 Figure 2). Error bars are the standard deviation of repeated triplicate measurements. The
186 performance of the liquid evaporation technique was validated by comparing the sensitivity to
187 dimethyl-1,1,1-d₃ sulfide (Praxair certified compressed gas standard, $0.184 \text{ ppm} \pm 10\%$) diluted by
188 zero air to a desired mixing ratio, with that of a diluted nebulized solution of DMS. The slope of
189 the linear fit for calibration measurements from the pressurized cylinder (DMS-d₃, $65 m/Q$) and
190 the solution (DMS, $62 m/Q$) agreed to better than 10%.

191

192 3. Results and Discussion

193 3.1 Benzene Cluster Cation Mass Spectra

194 The CI-ToFMS mass spectra, obtained while overflowing the inlet with nominally dry zero air is
195 shown in Figure 3a. To maximize the transmission of weakly bound ion-molecule adducts, we
196 operated the instrument in all of the experiments described here with a minimal applied electric
197 field between the instrument inlet and the entrance of the second RF-only quadrupole ion guide.
198 The two primary peaks in the mass spectrum correspond to the benzene cation (C_6H_6^+ ; $78 m/Q$)
199 and the benzene cation clustered to a single, neutral benzene ($\text{C}_6\text{H}_6^+ \cdot (\text{C}_6\text{H}_6)$; $156 m/Q$), where
200 C_6H_6^+ and $\text{C}_6\text{H}_6^+ \cdot (\text{C}_6\text{H}_6)$ combined account over 90% of the total ion current (TIC) for a benzene
201 neutral concentration of 300 ppm. Benzene cation clusters larger than the dimer were not observed,
202 as expected from their dissociation enthalpy, which is significantly smaller than that of the benzene
203 cation clustered with a single neutral benzene molecule (Krause et al., 1991). The observed mass
204 spectrum indicates significant ion intensity at 39, 50, 51, and 52 m/Q that are attributed to the
205 dissociation of the molecular (C_6H_6^+) ion into its fragments C_3H_3^+ , C_4H_2^+ , C_4H_3^+ , and C_4H_4^+ ,
206 accounting for ca. 5% of TIC. The fragmentation may result from the interaction of N_2^+ , α -particles
207 or electrons with benzene clusters in the ion molecule reaction region (Lifshitz and Reuben, 1969;



208 Talebpour et al., 2000). For comparison, a similar spectrum is shown in Figure 3b, using the same
209 benzene neutral concentration and operating voltages, but without the first RF-only quadrupole
210 ion guide. In this mode of operation, the total ion current is reduced by over 95%, and $C_6H_6^+$ and
211 $C_6H_6^+(C_6H_6)$ are nearly equal in intensity, highlighting that benzene cluster collisional
212 dissociation is occurring within this region. Even with the first RF-only quadrupole off, the $n=2$
213 cluster ($C_6H_6^+(C_6H_6)_2$; $234 m/Q$) was not observed. Of notable absence ($< 1\%$ TIC) in both Figures
214 3a and 3b are the organic contaminants (92, 106, and $120 m/Q$) previously attributed to alkyl
215 substituted benzene and protonated water clusters ($H_3O^+(H_2O)_n$; 19, 37, 55, and $73 m/Q$) that were
216 present at high abundance ($>10\%$ of TIC) in Kim et al. (2016). It was postulated in Kim et al., that
217 the source of the organic contaminants was the benzene compressed gas cylinder, as their
218 combined contribution to TIC scaled with the neutral benzene concentration. It was also noted that
219 low benzene neutral concentrations led to elevated water cluster abundance. This resulted in an
220 optimum benzene neutral concentration of 10 ppm, to balance the contributions from organic
221 contaminants and water clusters. Here, we eliminate the organic contaminants through the use of
222 a high purity benzene liquid source permitting operation at higher neutral benzene concentrations
223 (> 300 ppm). As discussed in section 3.2, this has critical advantages for the detection of analytes
224 such as isoprene, and effectively eliminates competing ion chemistry stemming from protonated
225 water clusters.

226 It what follows we assess the CI-ToFMS sensitivity to a series of terpenes, including isoprene, α -
227 pinene, β -pinene, D-limonene, ocimene, β -myrcene, farnesene, α -humulene, β -caryophyllene, and
228 isolongifolene at atmospherically relevant mixing ratios (< 100 pptv) and determine the
229 dependence of CI-ToFMS sensitivity on the reagent ion neutral delivery concentration (section
230 3.2) and water vapor concentration (section 3.3).

231 3.2 Impact of Benzene Neutral Concentration on Terpene Sensitivity

232 We examined the impact of the benzene reagent ion precursor concentration on terpene sensitivity
233 in nominally dry zero air for benzene neutral concentrations between 60-300 ppm. For the selection
234 of monoterpenes and sesquiterpenes studied here, there was no indication that instrument
235 sensitivity was dependent on the neutral benzene reagent ion precursor concentration between 60–
236 300 ppm (Figure 4 a-b). In Figure 4a-c, the reported sensitivity for each terpene is normalized to
237 that measured at a benzene neutral concentration of 300 ppm. Unlike MTs and SQTs, the



238 sensitivity of the isoprene benzene adduct ($C_6H_6^+ \cdot C_5H_8$; 146 m/Q) strongly depends on the benzene
239 concentration below 200 ppm (Figure 4 c) and therefore all the measurements in this study, were
240 conducted at 300 ppm benzene. The cause for this dependence in benzene concentration is unclear
241 as the exact mechanism for $C_6H_6^+ \cdot C_5H_8$ formation is unknown. It should also be noted that the
242 sensitivity to DMS is independent of benzene concentration. Based on these analyses, we suggest
243 that future studies utilizing benzene ion chemistry operate at neutral benzene reagent ion precursor
244 concentrations of 300 ppm, generated from a high purity liquid source.

245

246 3.3 Impact of Specific Humidity on Sensitivity

247 3.3.1 Isoprene

248 In these experiments, the specific humidity (SH) was varied between 0 and 14 $g\ kg^{-1}$, equivalent
249 to 0-80% RH at 23°C, to assess its effect on the sensitivity. Our reported “nominally dry” cases
250 correspond to 0.7% RH or ca. 0.01 $g\ kg^{-1}$ SH. As shown in Figure 5, the sensitivity of the CI-
251 ToFMS to isoprene ($C_6H_6^+ \cdot C_5H_8$; 146 m/Q) displays a strong, non-linear dependence on SH.
252 Instrument sensitivity increases with increasing SH, reaching a maximum value of 10 $ncps \cdot ppt^{-1}$
253 at 4 $g\ kg^{-1}$ (25% RH at 23°C), then decreases significantly at higher humidity. Surprisingly, we
254 observed a linear correlation ($R^2 > 0.95$) between the protonated water tetramer signal (73 m/Q)
255 and the delivered isoprene mixing ratio at constant SH that was not observed for smaller protonated
256 water clusters (Figure 6). The apparent sensitivity, derived from the slope of the linear-least
257 squares fit of the observed water tetramer signal vs. delivered isoprene concentration, increases
258 with increasing specific humidity above 2 $g\ kg^{-1}$ (Figure 5). We reiterate that Figure 5 does not
259 show the protonated tetramer signal as a function of SH, but the *sensitivity* of the 73 m/Q signal to
260 the delivered isoprene mixing ratio as shown in Figure 6. The decreased sensitivity to isoprene
261 adduct and increase in water tetramer signal with isoprene mixing ratio are unlikely the result of
262 the formation of water protonated clusters *via* charge transfer reaction with benzene cations since
263 the IE of water is significantly higher than that of the benzene dimer (12.62 and 8.69 eV
264 respectively). Since the formation of water tetramer clusters increases with isoprene mixing ratio
265 and humidity, it is suggested that the interaction between water clusters and isoprene-benzene
266 adducts in the IMR results in a charge exchange from the isoprene-adduct to the water tetramer in
267 a similar way that was previously described between benzene cation and water clusters. For
268 example, Ibrahim *et al.* (2005) showed that the IR spectra of benzene-water ion clusters



269 $[(\text{H}_2\text{O})_n\text{C}_6\text{H}_6]^+$ where ($n \geq 4$) resembles that of protonated water clusters and suggested that the
270 charge is held by the water molecules, such clusters that are likely to be formed in the IMR are
271 expected to be broken apart in the ion optics. It is likely that the observed trends of the humidity
272 dependent sensitivity of isoprene and water tetramer signal also results from a similar formation
273 and de-clustering in our CI-ToFMS.

274 3.3.2 Monoterpenes

275 The dependence of monoterpene sensitivity on SH is shown in Figure 7 for the molecular ion
276 ($\text{C}_{10}\text{H}_{16}^+$; 136 m/Q). Instrument sensitivity under nominally dry conditions displays a wide range
277 of sensitivities, that are species dependent (4.8 to $21.0\text{ ncps}\cdot\text{ppt}^{-1}$). At high specific humidity,
278 sensitivities converge significantly (9.5 to $15.0\text{ ncps}\cdot\text{ppt}^{-1}$). The observed dependence in the α -
279 pinene sensitivity on SH reported here is counter to that previously reported by our group in Kim
280 et al. (2016). This is attributed to the different instrument operational configuration used here (e.g.,
281 high concentration and purity benzene reagent ion precursor and low electric field strengths).

282 The humidity dependent sensitivity of D-limonene is anomalous compared with the other
283 monoterpenes studied, where the CI-ToFMS sensitivity to D-limonene decreases by a factor of 4
284 over the studied humidity range. The gradual and systematic decrease of the sensitivity suggests
285 that the ionization of D-limonene by charge transfer is not the only ionization mechanism and/or
286 that the D-limonene cation is subjected to subsequent reactions which results in the formation of
287 other detectable ions. We calculated the calibration curves of each of the recorded mass-to-charge
288 ratios to identify product ions that showed: 1) high correlation with the delivered D-limonene
289 mixing ratio ($R^2 > 0.98$) and 2) the contribution to the total sensitivity (i.e. slope) was higher than
290 1 ncps ppt^{-1} . A representative normalized calibration curve of the three ions (135, 136, and 168
291 m/Q) that met these criteria is presented in Figure 8. The peak at 168 m/Q ($\text{C}_{10}\text{H}_{16}\text{O}_2^+$) is attributed
292 to either a D-limonene- O_2 adduct or a D-limonene oxidation product (e.g. limonene epoxide). The
293 peak at 135 m/Q ($\text{C}_{10}\text{H}_{15}^+$) represent the $[\text{M}-1]^+$ product, perhaps due to rearrangements of the
294 molecular ion. The purity of the primary standard was confirmed *via* GC-MS, and comparable
295 peak ratios were measured when sampling the standard directly, ruling out the potential for the
296 nebulization process to alter the MS peak ratios. Finally, the $[\text{M}+32]^+$ peak intensity is reduced to
297 baseline by sampling the terpene in nitrogen, suggesting that the $[\text{M}+32]^+$ peak is a result of
298 secondary ion chemistry involving O_2 . The normalized sensitivity of each of these three peaks



299 decreases with increasing SH (Figure 9), suggesting that water clusters compete or suppress the
300 charge transfer to the contributing ions. The humidity dependent sensitivity of all the studied MTs,
301 calculated as the sum of all their contributing ions, shows lower variability, mostly due to the
302 higher sensitivity to D-limonene when all product ions are accounted for (Figure 10). The
303 variations in the sensitivities between different monoterpenes is small (14 ± 3 ncps ppt⁻¹) and
304 instrumental response is largely independent on SH from 4 to 14 g kg⁻¹. This range is typical at
305 boreal forests during the summer (Suni et al., 2003).

306 3.3.3 Sesquiterpenes

307 The sensitivities of the CI-ToFMS toward SQTs, detected as the charge transfer product at 204
308 *m/Q*, show minimal dependence on SH between nominally dry conditions and 14 g kg⁻¹ (Figure
309 11). Using the same process discussed in section 3.3.2 for identifying other product ions, it was
310 found that 203 and 236 *m/Q* (C₁₅H₂₃⁺ and C₁₅H₂₄O₂⁺) also contributed to product ion intensity.

311 The response of the farnesene and isolongifolene molecular ions and their related contributing ions
312 are presented as examples of SQTs dependence on SH (Figure 12). All three major ions were
313 observed at all measured SHs and in the case of isolongifolene, the normalized response of 203
314 *m/Q* (C₁₅H₂₃⁺) was higher than the molecular ion (204 *m/Q*, C₁₅H₂₄⁺) over the entire SH range
315 including at nominally dry conditions (Figure 12). At present, we don't have a definitive
316 mechanism for the product ion distribution, but the presence of similar products (i.e. ([M-1]⁺ and
317 ([M+32]⁺) and their humidity dependence suggest that the molecular ions of sesquiterpenes are
318 subjected to similar reactions as MTs which results in a lower signal of the molecular ion. Similar
319 to MTs, the humidity dependent sensitivities of sesquiterpenes calculated as the sum of all
320 contributing ions, lowers the variability in calculated sensitivities (Figure 13). Since the sensitivity
321 is independent of the humidity a general sensitivity to all SQTs of 9.6 ± 2.3 ncps pptv⁻¹ can be
322 further used for quantification of ambient SQTs.

323

324 4. Conclusions

325 We show that benzene cluster cations are a sensitive reagent ion for chemical ionization of select
326 biogenic volatile organic compounds. We demonstrate that isoprene is primarily detected as an
327 adduct (C₅H₈·C₆H₆⁺) with a sensitivity ranging between 4-10 ncps ppt⁻¹, that depends strongly on



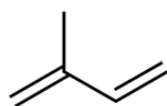
328 the reagent ion precursor concentration, de-clustering voltages, and specific humidity (SH). This
329 highlights the importance of continuous infield calibrations for isoprene concentration
330 measurements. We show that monoterpenes are primarily detected as the molecular ion ($C_{10}H_{16}^+$)
331 with an average sensitivity, across the five measured compounds, of 14 ± 3 ncps ppt⁻¹ for SH
332 between 7 and 14 g kg⁻¹, typical of the boreal forest during summer. Sesquiterpenes are detected
333 primarily as the molecular ion ($C_{15}H_{24}^+$) with an average sensitivity, across the four measured
334 compounds, of 9.6 ± 2.3 ncps ppt⁻¹ that is also independent of specific humidity. We suggest that
335 future studies that utilize benzene cluster cation chemistry use high purity liquid reservoirs and
336 benzene neutral concentrations at or above 300 ppmv.

337 **Acknowledgements**

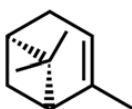
338 This work was supported by a National Science Foundation (NSF) CAREER Award (Grant No.
339 AGS-1151430) and the Office of Science (Office of Biological and Environmental Research), U.S.
340 Department of Energy (Grant No. DE-SC0006431). A.L. gratefully acknowledges support from
341 the Dreyfus Foundation Environmental Chemistry Postdoctoral Fellowship Program.



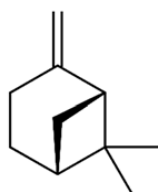
342 **Table 1. Molecular structures for the terpenes characterized in this study.**



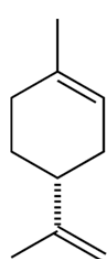
isoprene



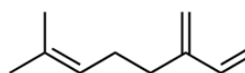
α -pinene



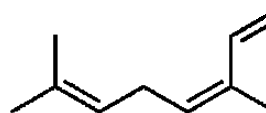
β -pinene



D-limonene



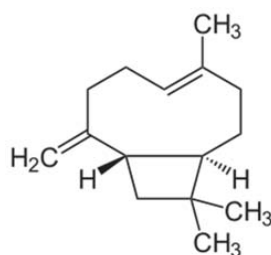
β -myrcene



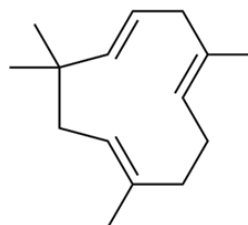
ocimene



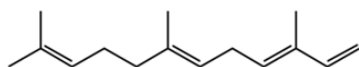
isolongifolene



β -caryophyllene



α -humulene



farnesene

343

344

345 **Table 2. Monoterpene sensitivities and dependence on operating and sampling conditions.**

Compound	Sensitivity [†] (ncps pptv ⁻¹) (SH = 6.9 g kg ⁻¹)	M ⁺ : [M-1] ⁺ : [M+32] ⁺ (SH = 0.01 g kg ⁻¹) [‡]	M ⁺ : [M-1] ⁺ : [M+32] ⁺ (SH = 6.9 g kg ⁻¹) [‡]	f(H ₂ O)	f(C ₆ H ₆)
α-pinene	17.9	23.9:0.64:0.35	17.4:0.21:0.25	Y	N
β-pinene	18.4	14.9:0.28:0.33	17.6:0.33:0.39	N	N
D-limonene	13.6	5.4:3.4:8.0	3.7:3.0:6.9	Y	N
β-myrcene	11.5	4.6:0.56:0.94	8.7:1.1:1.7	Y	N
ocimene	13.2	13.1:1.50:0.29	12.4:0.42:0.36	N	N

346 [†]SH = 6.9 g kg⁻¹ corresponds to 65 % RH at 15 °C, representative of Boreal regions. The reported
 347 sensitivity includes the contributions from the M⁺, M-1⁺, and M+32⁺ ions.

348 [‡]Sensitivities (ncps pptv⁻¹) at M⁺, M-1⁺, and M+32⁺, is reported for SH = 0.01 and 6.9 g kg⁻¹.

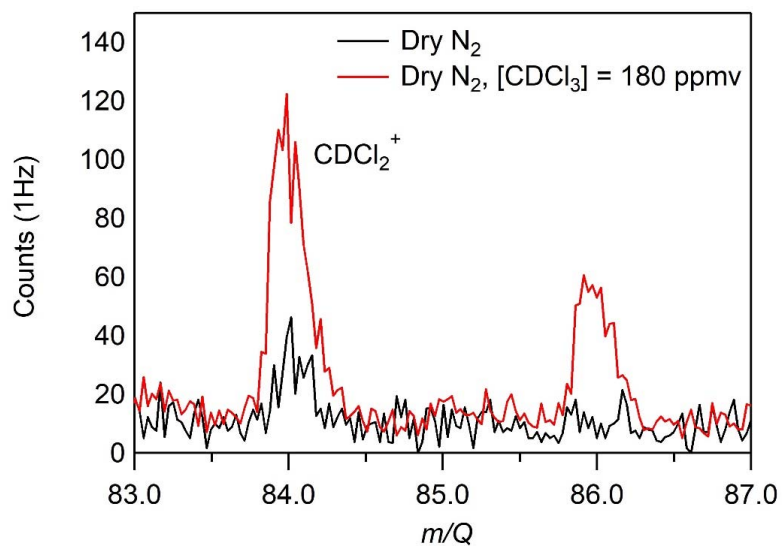
349

350 **Table 3. Sesquiterpene sensitivities and dependence on operating and sampling conditions.**

Compound	Sensitivity [†] (ncps pptv ⁻¹) (SH = 6.9 g kg ⁻¹)	M ⁺ : [M-1] ⁺ : [M+32] ⁺ (SH = 0.01 g kg ⁻¹) [‡]	M ⁺ : [M-1] ⁺ : [M+32] ⁺ (SH = 6.9 g kg ⁻¹) [‡]	f(H ₂ O)	f(C ₆ H ₆)
farnesene	10.4	7.8:1.3:1.6	7.8:1.:1:1.5	Y	N
α-humulene	8.6	5.2:2.6:0.63	1:5.3:2.8:0.54	N	N
β-caryophellene	6.9	4.6:1.4:2.2	4.0:1.1:1.9	Y	N
isolongifolene	12.3	3.1:7.7:1.2	3.4:8.8:0.15	Y	N

351 [†]SH = 6.9 g kg⁻¹ corresponds to 65 % RH at 15 °C, representative of Boreal regions. The reported
 352 sensitivity includes the contributions from the M⁺, M-1⁺, and M+32⁺ ions.

353 [‡]Sensitivities (ncps pptv⁻¹) at M⁺, M-1⁺, and M+32⁺, is reported for SH = 0.01 and 6.9 g kg⁻¹.

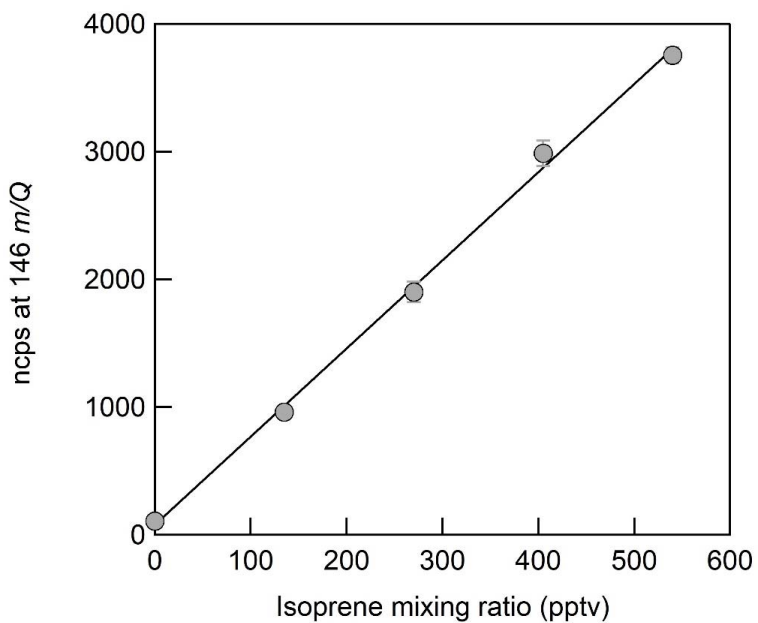


354

355

356

357 **Figure 1.** CI-ToFMS mass spectrum acquired when overflowing the inlet with excess nitrogen358 (black) and for a nebulized solution of chloroform-d at a flow rate of $3\mu\text{l min}^{-1}$ in a nitrogen carrier359 gas (red), where the resulting $[\text{CDCl}_3] = 180\text{ ppmv}$. No signal was observed above the baseline for360 any other fragments or the parent (CDCl_3^+ , 120 m/Q).

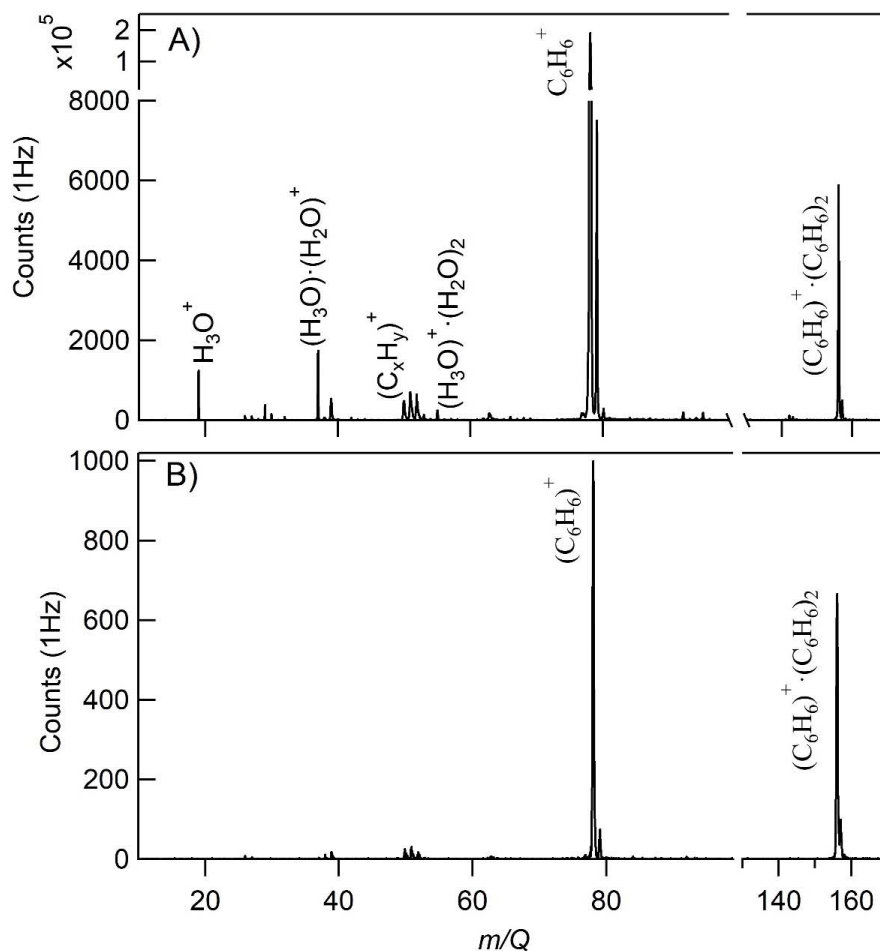


361
362

363 **Figure 2.** CI-ToFMS calibration curve for isoprene, detected as $C_6H_6^+ \cdot C_5H_8$ at 146 m/Q . The
364 sensitivity (slope) is 7 ncps, $R^2=0.99$. Error bars represents the standard deviation of the 1Hz
365 measurements.
366



367



368

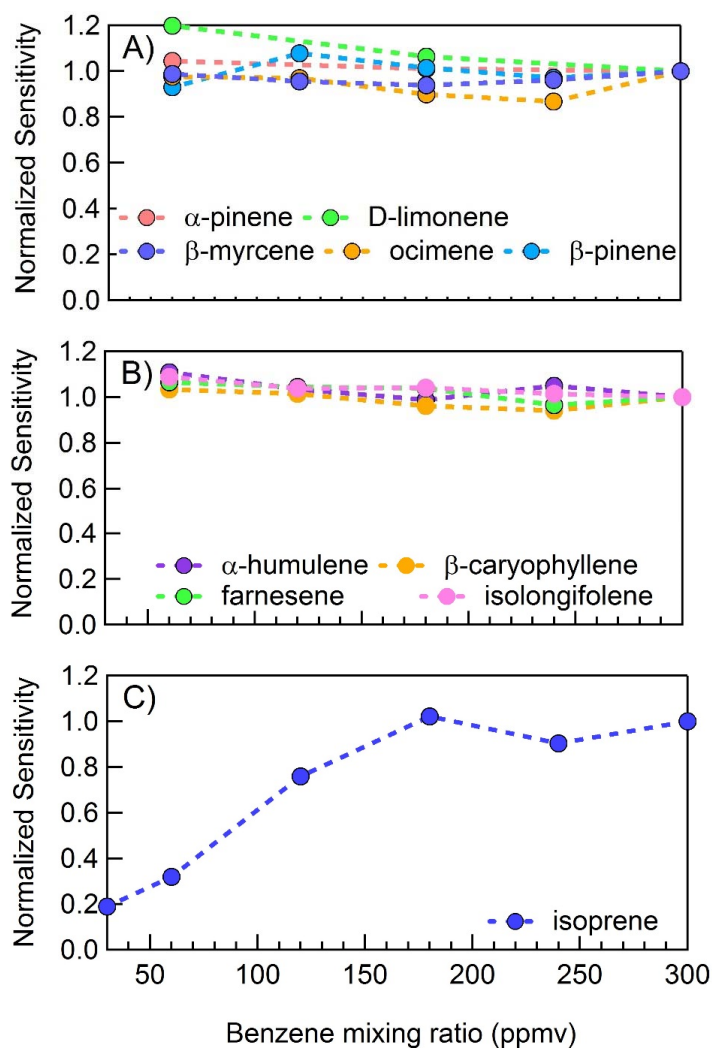
369 **Figure 3.** a) CI-ToFMS mass spectrum acquired when overflowing the inlet with nominally dry

370 zero air for a benzene neutral concentration of 300 ppm using a liquid reagent ion delivery and b)

371 same as in a, but with the first RF-only octupole ion guide turned off, resulting in a much weaker

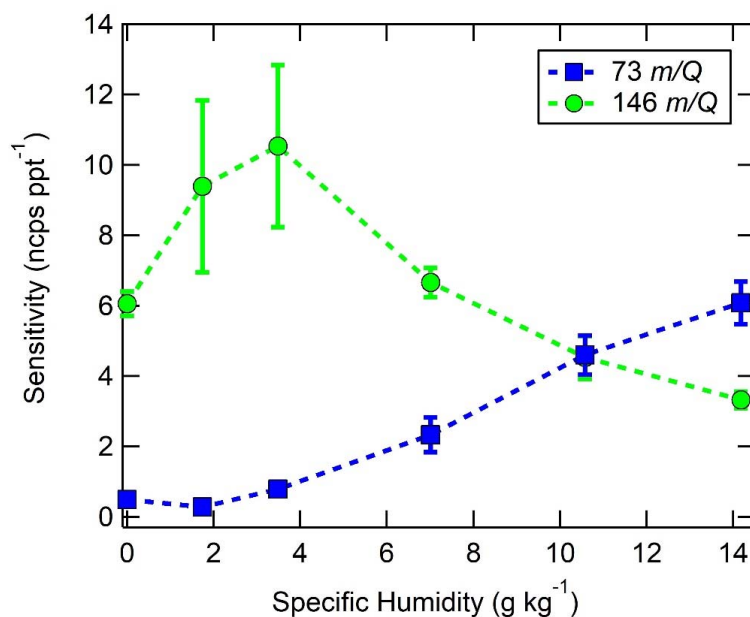
372 electric field strength.

373



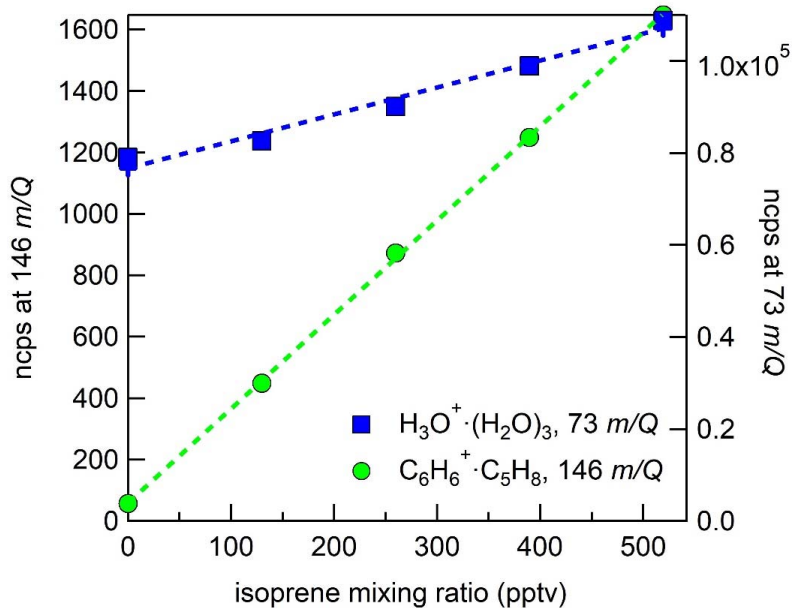
374

375 **Figure 4.** CI-ToFMS sensitivity to: a) monoterpenes ($C_{10}H_{15}^+$; 136 m/Q), b) sesquiterpenes
376 ($C_{15}H_{24}^+$; 204 m/Q), and c) isoprene ($C_6H_6^+ \cdot C_5H_8$; 146 m/Q) as a function of benzene neutral
377 concentration normalized to the sensitivity at 300 ppmv neutral benzene. Measurements were
378 conducted in nominally dry zero air.
379



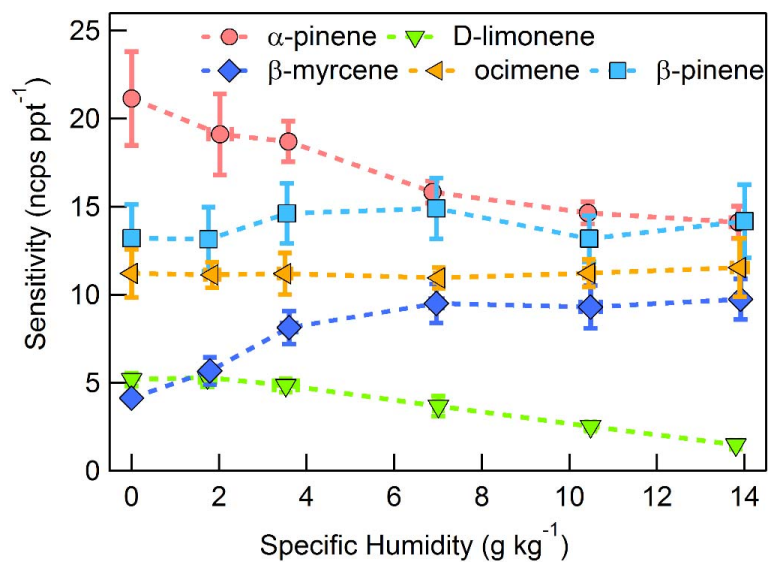
380

381 **Figure 5.** Humidity dependent CI-ToFMS sensitivities to isoprene (green circles, $C_6H_6^+ \cdot C_5H_8$, 146
382 m/Q), and the protonated water tetramer (blue squares, $H_3O^+ \cdot (H_2O)_3$, 73 m/Q), derived from
383 calibration curves such as those shown in Figure 6. The reported sensitivities are the average of
384 triplicate calibration curves with all linear best fits having $R^2 > 0.98$. Error bars represent the
385 standard deviation of the triplicate calibrations. All calibrations were performed in zero air.
386



387
388
389
390
391
392

Figure 6. CI-ToFMS sensitivity to isoprene, observed as the isoprene-benzene cluster (green circles, $C_6H_6^+ \cdot C_5H_8$, $146\ m/Q$) and water protonated tetramer (blue squares, $H_3O^+ \cdot (H_2O)_3$, $73\ m/Q$). Dashed lines are the least square best fit lines ($R^2 > 0.98$). Calibration was performed at SH of $14\ g\ kg^{-1}$ in zero air.

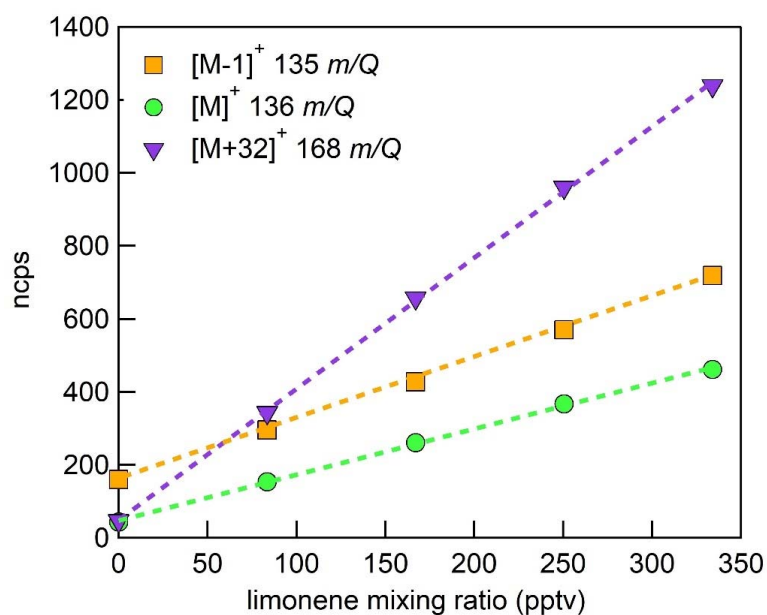


393

394 **Figure 7.** Humidity dependent sensitivities to select MTs detected as M^+ ($C_{10}H_{16}^+$, $136\ m/Q$). Error
395 bars indicate the standard deviation of triplicate measurements. All calibrations were conducted in
396 zero air. Error bars represent the standard deviation of the triplicate calibrations. All calibrations
397 were performed in zero air.
398

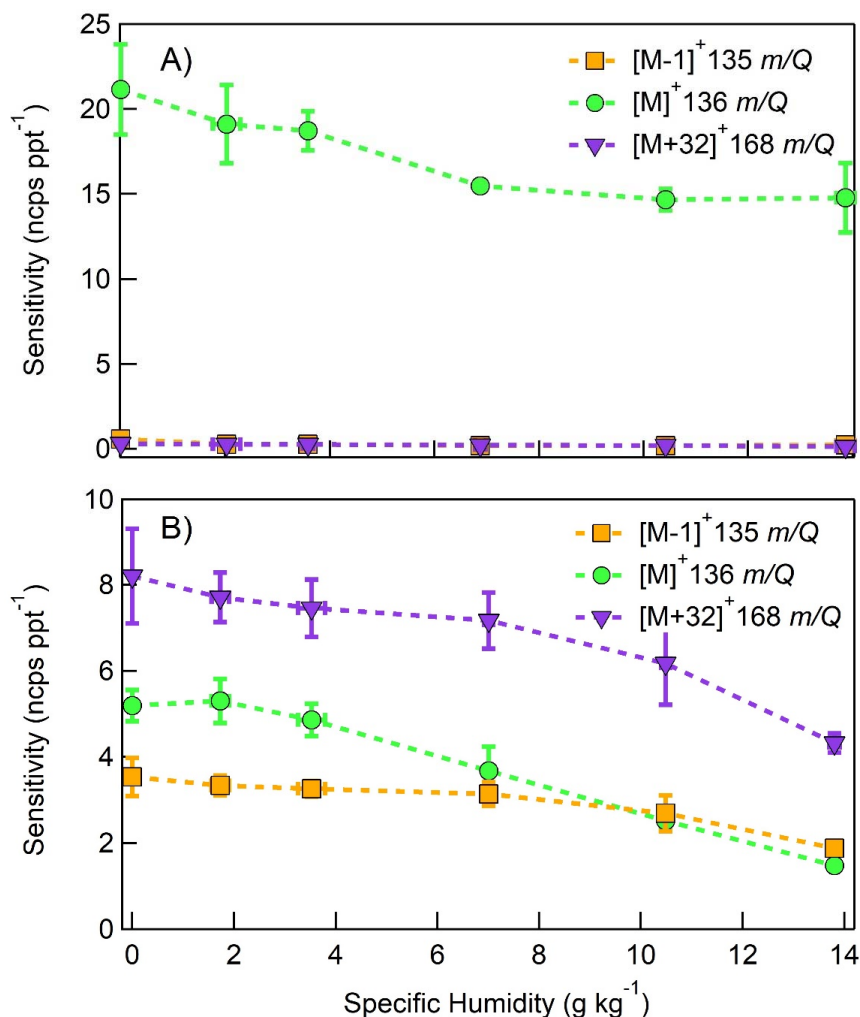


399



400

401 **Figure 8.** Normalized calibration of D-limonene for all major product ions ($C_{10}H_{16}^+$, 136 m/Q ,
402 green circles), ($C_{10}H_{15}^+$, 135 m/Q , orange squares), and ($C_{10}H_{16}O_2^+$, 168 m/Q , purple triangles).
403 Calibration was performed in zero air at 14 $g\ kg^{-1}$ specific humidity (80% RH at 23°C). Dashed
404 lines are least squares best fit lines (all $R^2 > 0.99$).
405

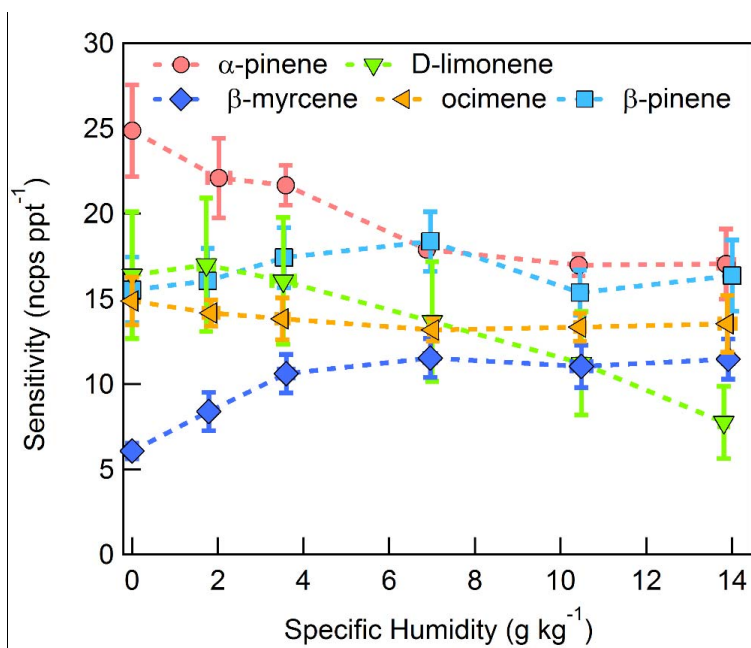


406

407 **Figure 9.** Humidity dependent, normalized sensitivities to a) α -pinene b) D-limonene for all major
408 product ions ($\text{C}_{10}\text{H}_{16}^+$, 136 m/Q , green circles), ($\text{C}_{10}\text{H}_{15}^+$, 135 m/Q , orange squares), and
409 ($\text{C}_{10}\text{H}_{16}\text{O}_2^+$, 168 m/Q , purple triangles). Error bars represent the standard deviation of the triplicate
410 calibrations. All calibrations were performed in zero air.
411



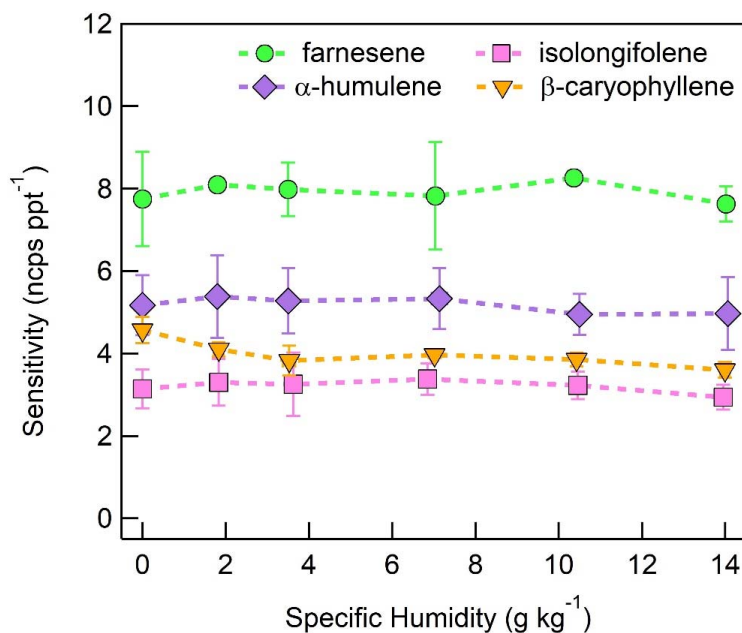
412



413

414 **Figure 10.** Humidity dependent, CI-ToFMS monoterpene sensitivities reported as the sum of all
 415 detected masses (135, 136, and 168 m/Q). Error bars represent the standard deviation of the
 416 triplicate calibrations. All calibrations were performed in zero air.

417

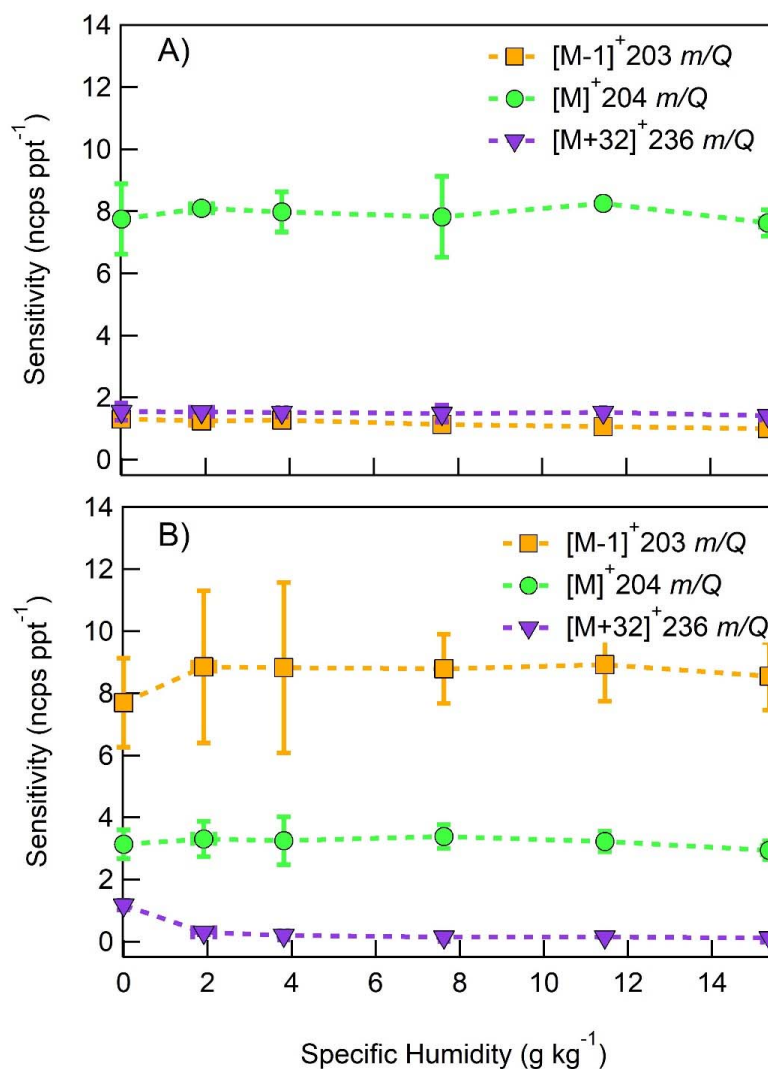


418

419 **Figure 11.** Humidity dependent sensitivities of SQTs detected as C₁₅H₂₄ (204 *m/Q*). Error bars
 420 represent the standard deviation of triplicate measurements. All calibrations were performed in
 421 zero air.



422



423

424

425

426

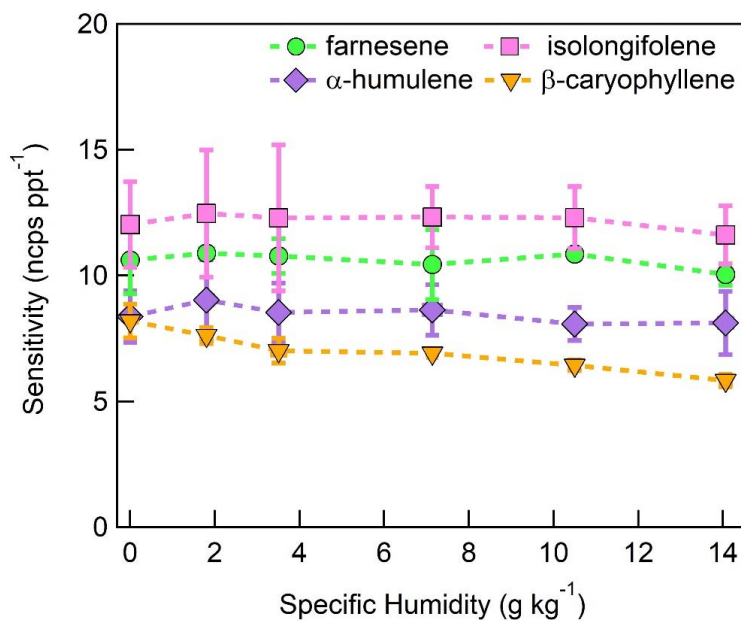
427

428

429

430

Figure 12. Humidity dependent, normalized sensitivities to a) farnesene and b) isolongifolene for all major product ions ($C_{15}H_{23}^+$, 203 m/Q , orange squares), ($C_{15}H_{24}^+$, 204 m/Q , green circles), and ($C_{15}H_{24}O_2^+$, 236 m/Q , purple triangles). Error bars represent the standard deviation of the triplicate measurement.



431

432 **Figure 13.** Humidity dependent, normalized sensitivities to sesquiterpenes, reported as the sum of
 433 the major product ions ($C_{15}H_{23}^+$, 203 m/Q), ($C_{15}H_{24}^+$, 204 m/Q), and ($C_{15}H_{24}O_2^+$, 236 m/Q). Error
 434 bars represent the standard deviation of triplicate measurements.

435

436 **References**

- 437 Allan, J. D., Alfarra, M. R., Bower, K. N., Coe, H., Jayne, J. T., Worsnop, D. R., Aalto, P. P., Kulmala, M.,
438 Hyötyläinen, T., Cavalli, F., and Laaksonen, A.: Size and composition measurements of background aerosol
439 and new particle growth in a Finnish forest during QUEST 2 using an Aerodyne Aerosol Mass Spectrometer,
440 *Atmos. Chem. Phys.*, 6, 315-327, 2006.
- 441 Bertram, T. H., Kimmel, J. R., Crisp, T. A., Ryder, O. S., Yatavelli, R. L. N., Thornton, J. A., Cubison, M. J.,
442 Gonin, M., and Worsnop, D. R.: A field-deployable, chemical ionization time-of-flight mass spectrometer,
443 *Atmospheric Measurement Techniques*, 4, 1471-1479, 2011.
- 444 Bieri, G., Asbrink, L., and Vonniessen, W.: 30.4-Nm He(I) Photoelectron-Spectra of Organic-Molecules .4.
445 Fluoro-Compounds (C,H,F), *Journal of Electron Spectroscopy and Related Phenomena*, 23, 281-322, 1981.
- 446 Chipot, C., Jaffe, R., Maigret, B., Pearlman, D. A., and Kollman, P. A.: Benzene dimer: A good model for pi-
447 pi interactions in proteins? A comparison between the benzene and the toluene dimers in the gas phase
448 and in an aqueous solution, *Journal of the American Chemical Society*, 118, 11217-11224, 1996.
- 449 Chung, C. E., Ramanathan, V., and Decremier, D.: Observationally constrained estimates of carbonaceous
450 aerosol radiative forcing, *Proc Natl Acad Sci U S A*, 109, 11624-11629, 2012.
- 451 Crouse, J. D., McKinney, K. A., Kwan, A. J., and Wennberg, P. O.: Measurement of gas-phase
452 hydroperoxides by chemical ionization mass spectrometry, *Anal Chem*, 78, 6726-6732, 2006.
- 453 Dondes, S., Harbeck, P., and Kunz, C.: A Spectroscopic Study of Alpha-Ray-Induced Luminescence in Gases
454 .1., *Radiation Research*, 27, 174-8, 1966.
- 455 Greenspan, L.: Humidity Fixed-Points of Binary Saturated Aqueous-Solutions, *Journal of Research of the*
456 *National Bureau of Standards Section a-Physics and Chemistry*, 81, 89-96, 1977.
- 457 Grover, J. R., Walters, E. A., and Hui, E. T.: Dissociation-Energies of the Benzene Dimer and Dimer Cation,
458 *Journal of Physical Chemistry*, 91, 3233-3237, 1987.
- 459 Guenther, A., Hewitt, C. N., Erickson, D., Fall, R., Geron, C., Graedel, T., Harley, P., Klinger, L., Lerdau, M.,
460 McKay, W. A., Pierce, T., Scholes, B., Steinbrecher, R., Tallamraju, R., Taylor, J., and Zimmerman, P.: A
461 Global-Model of Natural Volatile Organic-Compound Emissions, *Journal of Geophysical Research-*
462 *Atmospheres*, 100, 8873-8892, 1995.
- 463 Guenther, A. B., Jiang, X., Heald, C. L., Sakulyanontvittaya, T., Duhl, T., Emmons, L. K., and Wang, X.: The
464 Model of Emissions of Gases and Aerosols from Nature version 2.1 (MEGAN2.1): an extended and updated
465 framework for modeling biogenic emissions, *Geoscientific Model Development*, 5, 1471-1492, 2012.
- 466 Hallquist, M., Wenger, J. C., Baltensperger, U., Rudich, Y., Simpson, D., Claeys, M., Dommen, J., Donahue,
467 N. M., George, C., Goldstein, A. H., Hamilton, J. F., Herrmann, H., Hoffmann, T., Iinuma, Y., Jang, M., Jenkin,
468 M. E., Jimenez, J. L., Kiendler-Scharr, A., Maenhaut, W., McFiggans, G., Mentel, T. F., Monod, A., Prevot,
469 A. S. H., Seinfeld, J. H., Surratt, J. D., Szmigielski, R., and Wildt, J.: The formation, properties and impact of
470 secondary organic aerosol: current and emerging issues, *Atmospheric Chemistry and Physics*, 9, 5155-
471 5236, 2009.
- 472 Huey, L. G.: Measurement of trace atmospheric species by chemical ionization mass spectrometry:
473 Speciation of reactive nitrogen and future directions, *Mass Spectrom Rev*, 26, 166-184, 2007.
- 474 Hunt, D. F. and Harvey, T. M.: Nitric oxide chemical ionization mass spectra of alkanes, *Analytical*
475 *Chemistry*, 47, 1965-1969, 1975.
- 476 Hunt, D. F., Harvey, T. M., Brumley, W. C., Ryan, J. F., and Russell, J. W.: Nitric oxide chemical ionization
477 mass spectrometry of alcohols, *Analytical Chemistry*, 54, 492-496, 1982.
- 478 Ibrahim, Y. M., Mautner, M. M. N., Alshraeh, E. H., El-Shall, M. S., and Scheiner, S.: Stepwise hydration of
479 ionized aromatics. Energies, structures of the hydrated benzene cation, and the mechanism of
480 deprotonation reactions, *J Am Chem Soc*, 127, 7053-7064, 2005.
- 481 IPCC: Climate Change 2013: The Physical Science Basis. Contribution of Working Group I to the Fifth
482 Assessment Report of the Intergovernmental Panel on Climate Change, Cambridge University Press, 2013.



- 483 Jokinen, T., Berndt, T., Makkonen, R., Kerminen, V. M., Junninen, H., Paasonen, P., Stratmann, F.,
484 Herrmann, H., Guenther, A. B., Worsnop, D. R., Kulmala, M., Ehn, M., and Sipila, M.: Production of
485 extremely low volatile organic compounds from biogenic emissions: Measured yields and atmospheric
486 implications, *Proc Natl Acad Sci U S A*, 112, 7123-7128, 2015.
- 487 Kerminen, V. M., Lihavainen, H., Komppula, M., Viisanen, Y., and Kulmala, M.: Direct observational
488 evidence linking atmospheric aerosol formation and cloud droplet activation, *Geophysical Research*
489 *Letters*, 32, 2005.
- 490 Kim, M. J., Farmer, D. K., and Bertram, T. H.: A controlling role for the air-sea interface in the chemical
491 processing of reactive nitrogen in the coastal marine boundary layer, *P Natl Acad Sci USA*, 111, 3943-3948,
492 2014.
- 493 Kim, M. J., Zoerb, M. C., Campbell, N. R., Zimmermann, K. J., Blomquist, B. W., Huebert, B. J., and Bertram,
494 T. H.: Revisiting benzene cluster cations for the chemical ionization of dimethyl sulfide and select volatile
495 organic compounds, *Atmospheric Measurement Techniques*, 9, 1473-1484, 2016.
- 496 Kim, S., Karl, T., Helmig, D., Daly, R., Rasmussen, R., and Guenther, A.: Measurement of atmospheric
497 sesquiterpenes by proton transfer reaction-mass spectrometry (PTR-MS), *Atmospheric Measurement*
498 *Techniques*, 2, 99-112, 2009.
- 499 Kirkby, J., Duplissy, J., Sengupta, K., Frege, C., Gordon, H., Williamson, C., Heinritzi, M., Simon, M., Yan, C.,
500 Almeida, J., Trostl, J., Nieminen, T., Ortega, I. K., Wagner, R., Adamov, A., Amorim, A., Bernhammer, A. K.,
501 Bianchi, F., Breitenlechner, M., Brilke, S., Chen, X., Craven, J., Dias, A., Ehrhart, S., Flagan, R. C., Franchin,
502 A., Fuchs, C., Guida, R., Hakala, J., Hoyle, C. R., Jokinen, T., Junninen, H., Kangasluoma, J., Kim, J., Krapf,
503 M., Kurten, A., Laaksonen, A., Lehtipalo, K., Makhmutov, V., Mathot, S., Molteni, U., Onnela, A., Perakyla,
504 O., Piel, F., Petaja, T., Praplan, A. P., Pringle, K., Rap, A., Richards, N. A., Riipinen, I., Rissanen, M. P., Rondo,
505 L., Sarnela, N., Schobesberger, S., Scott, C. E., Seinfeld, J. H., Sipila, M., Steiner, G., Stozhkov, Y., Stratmann,
506 F., Tome, A., Virtanen, A., Vogel, A. L., Wagner, A. C., Wagner, P. E., Weingartner, E., Wimmer, D., Winkler,
507 P. M., Ye, P., Zhang, X., Hansel, A., Dommen, J., Donahue, N. M., Worsnop, D. R., Baltensperger, U.,
508 Kulmala, M., Carslaw, K. S., and Curtius, J.: Ion-induced nucleation of pure biogenic particles, *Nature*, 533,
509 521-526, 2016.
- 510 Krause, H., Ernstberger, B., and Neusser, H. J.: Binding-Energies of Small Benzene Clusters, *Chemical*
511 *Physics Letters*, 184, 411-417, 1991.
- 512 Kulmala, M., Suni, T., Lehtinen, K. E. J., Dal Maso, M., Boy, M., Reissell, A., Rannik, Ü., Aalto, P., Keronen,
513 P., Hakola, H., Bäck, J., Hoffmann, T., Vesala, T., and Hari, P.: A new feedback mechanism linking forests,
514 aerosols, and climate, *Atmos. Chem. Phys.*, 4, 557-562, 2004.
- 515 Lang-Yona, N., Rudich, Y., Mentel, T. F., Bohne, A., Buchholz, A., Kiendler-Scharr, A., Kleist, E., Spindler, C.,
516 Tillmann, R., and Wildt, J.: The chemical and microphysical properties of secondary organic aerosols from
517 Holm Oak emissions, *Atmospheric Chemistry and Physics*, 10, 7253-7265, 2010.
- 518 Leibrock, E. and Huey, L. G.: Ion chemistry for the detection of isoprene and other volatile organic
519 compounds in ambient air, *Geophysical Research Letters*, 27, 1719-1722, 2000.
- 520 Lifshitz, C. and Reuben, B. G.: Ion-Molecule Reactions in Aromatic Systems .I. Secondary Ions and Reaction
521 Rates in Benzene, *Journal of Chemical Physics*, 50, 951-&, 1969.
- 522 Lindinger, W., Hansel, A., and Jordan, A.: On-line monitoring of volatile organic compounds at pptv levels
523 by means of proton-transfer-reaction mass spectrometry (PTR-MS) - Medical applications, food control
524 and environmental research, *International Journal of Mass Spectrometry*, 173, 191-241, 1998.
- 525 Lopez-Hilfiker, F. D., Mohr, C., Ehn, M., Rubach, F., Kleist, E., Wildt, J., Mentel, T. F., Carrasquillo, A. J.,
526 Daumit, K. E., Hunter, J. F., Kroll, J. H., Worsnop, D. R., and Thornton, J. A.: Phase partitioning and volatility
527 of secondary organic aerosol components formed from alpha-pinene ozonolysis and OH oxidation: the
528 importance of accretion products and other low volatility compounds, *Atmospheric Chemistry and*
529 *Physics*, 15, 7765-7776, 2015.



- 530 Novak, I., Kovac, B., and Kovacevic, G.: Electronic structure of terpenoids, *Journal of Organic Chemistry*,
531 66, 4728-4731, 2001.
- 532 Riedel, T. P., Bertram, T. H., Crisp, T. A., Williams, E. J., Lerner, B. M., Vlasenko, A., Li, S. M., Gilman, J., de
533 Gouw, J., Bon, D. M., Wagner, N. L., Brown, S. S., and Thornton, J. A.: Nitryl Chloride and Molecular
534 Chlorine in the Coastal Marine Boundary Layer, *Environmental Science & Technology*, 46, 10463-10470,
535 2012.
- 536 Shinohara, H. and Nishi, N.: Excited-State Lifetimes and Appearance Potentials of Benzene Dimer and
537 Trimer, *Journal of Chemical Physics*, 91, 6743-6751, 1989.
- 538 Suni, T., Rinne, J., Reissell, A., Altimir, N., Keronen, P., Rannik, U., Dal Maso, M., Kulmala, M., and Vesala,
539 T.: Long-term measurements of surface fluxes above a Scots pine forest in Hyytiälä, southern Finland,
540 1996-2001, *Boreal Environment Research*, 8, 287-301, 2003.
- 541 Talebpour, A., Bandrauk, A. D., Vijayalakshmi, K., and Chin, S. L.: Dissociative ionization of benzene in
542 intense ultra-fast laser pulses, *Journal of Physics B-Atomic Molecular and Optical Physics*, 33, 4615-4626,
543 2000.
- 544 Thornton, J. A., Kercher, J. P., Riedel, T. P., Wagner, N. L., Cozic, J., Holloway, J. S., Dube, W. P., Wolfe, G.
545 M., Quinn, P. K., Middlebrook, A. M., Alexander, B., and Brown, S. S.: A large atomic chlorine source
546 inferred from mid-continental reactive nitrogen chemistry, *Nature*, 464, 271-274, 2010.
- 547 Werner, A. S., Tsai, B. P., and Baer, T.: Photoionization study of the ionization potentials and fragmentation
548 paths of the chlorinated methanes and carbon tetrabromide, *The Journal of Chemical Physics*, 60, 3650-
549 3657, 1974.
- 550 Wiedensohler, A., Cheng, Y. F., Nowak, A., Wehner, B., Achtert, P., Berghof, M., Birmili, W., Wu, Z. J., Hu,
551 M., Zhu, T., Takegawa, N., Kita, K., Kondo, Y., Lou, S. R., Hofzumahaus, A., Holland, F., Wahner, A., Gunthe,
552 S. S., Rose, D., Su, H., and Pöschl, U.: Rapid aerosol particle growth and increase of cloud condensation
553 nucleus activity by secondary aerosol formation and condensation: A case study for regional air pollution
554 in northeastern China, *Journal of Geophysical Research: Atmospheres*, 114, n/a-n/a, 2009.
- 555 Zhao, D. F., Buchholz, A., Tillmann, R., Kleist, E., Wu, C., Rubach, F., Kiendler-Scharr, A., Rudich, Y., Wildt,
556 J., and Mentel, T. F.: Environmental conditions regulate the impact of plants on cloud formation, *Nature*
557 *Communications*, 8, 2017.

558